Enrichment of Semiconducting Single-Walled Carbon Nanotubes by Carbothermic Reaction for Use in All-Nanotube Field Effect Transistors

Shisheng Li, Chang Liu,* Peng-Xiang Hou, Dong-Ming Sun, and Hui-Ming Cheng

Shenyang National Laboratory for Materials Science, Institute of Metal Research, Chinese Academy of Sciences, 72 Wenhua Road, Shenyang 110016, People's Republic of China

ABSTRACT

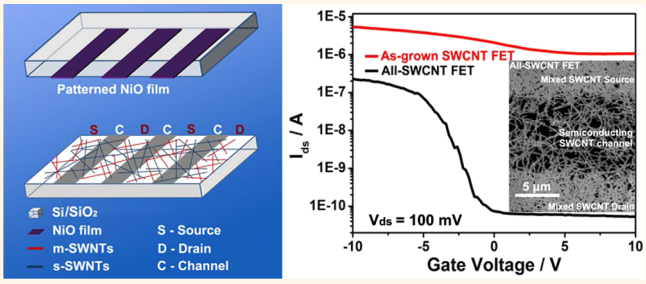

Selective removal of metallic single-walled carbon nanotubes (SWCNTs) and consequent enrichment of semiconducting SWCNTs were achieved through an efficient carbothermic reaction with a NiO thin film at a relatively low temperature of 350 °C. All-SWCNT field effect transistors (FETs) were fabricated with the aid of a patterned NiO mask, in which the as-grown SWCNTs behaving as source/drain electrodes and the remaining semiconducting SWCNTs that survive in the carbothermic reaction as a channel material. The all-SWCNT FETs demonstrate improved current ON/OFF ratios of $\sim 10^3$.

KEYWORDS: single-walled carbon nanotubes · carbothermic reaction · field effect transistors

Single-walled carbon nanotubes (SWCNTs) are promising for use in future electronics due to their extremely high carrier mobility[1] and current-carrying capacity,[2] ballistic transport,[3] and simple electrostatic current modulation with high ON/OFF ratios.[4] However, a key step in fabricating high performance SWCNT-based field effect transistors (FETs) is to obtain pure semiconducting SWCNTs (s-SWCNTs) avoiding electrical short circuits by metallic SWCNTs (m-SWCNTs). However, as-grown SWCNT samples are usually a mixture of s-SWCNTs and m-SWCNTs. Therefore, great efforts have been devoted to the selective preparation of pure s-SWCNTs and m-SWCNTs by *in situ* growth,[5−10] postsynthesis separation,[11,12] chemical modification,[13−16] electrical breakdown,[17,18] e-beam/light irradiation,[19,20] gas phase reaction,[21−23] *etc.* Although notable progress has been made in recent years, the efficiency and reproducibility in the enrichment of s-SWCNTs still need to be improved due to a poor overall performance of the fabricated devices. For example, postsynthesis separation and chemical modification tend to cause contaminations and structural defects of the as-grown SWCNTs which are detrimental to their performance. Electrical breakdown is highly effective but time-consuming, and cannot be scalable to systems with millions or billions of transistors. On the other hand, e-beam/light irradiation and gas phase reaction are either time-consuming or suffering from reversible metallic-to-semiconducting transition and instability of the device performance.

In the present work, we report the selective removal of m-SWCNTs by a carbothermic reaction method. Because of their preferential reaction with NiO thin film, m-SWCNTs can be selectively etched at a relatively low temperature of 350 °C. Furthermore, all-SWCNT FETs using as-grown SWCNTs as source/drain electrodes and the remaining s-SWCNTs that survive the carbothermic reaction as a channel material were fabricated with the aid of a patterned NiO mask. These FETs show current ON/OFF ratios of $\sim 10^3$. More importantly, such all-SWCNT FETs may find applications in various flexible devices.

Carbothermic reactions are widely used for refining metals, such as Fe and Al, from their oxide minerals. During this process, metal oxides are reduced to metals, while

* Address correspondence to cliu@imr.ac.cn.

Received for review July 10, 2012 and accepted October 1, 2012.

Published online October 01, 2012
10.1021/nn303070p

carbon is oxidized to CO or CO_2. Since m-SWCNTs are chemically more reactive than s-SWCNTs due to their smaller ionization potential,[6,9,13,22] we propose removing m-SWCNTs selectively by using a carbothermic reaction with NiO. We selected NiO as the oxidant because of its appropriate reduction potential,[24] which makes m-SWCNTs efficiently removed while s-SWCNTs are retained under the optimum oxidation conditions.

RESULTS AND DISCUSSION

Figure 1 schematically illustrates the process of removing m-SWCNTs by the carbothermic reaction. First, a 100 nm-thick Ni film was sputtered onto a Si/SiO_2 substrate and then oxidized at 600 °C under an ambient atmosphere. Scanning electron microscopy (SEM) observation and X-ray photoelectron spectroscopy (XPS) analysis confirmed the formation of NiO film after the thermal oxidation (Figure S1, Supporting Information). Second, a Si/SiO_2 substrate coated with the NiO film was placed on another Si/SiO_2 substrate with SWCNTs grown on its surface by chemical vapor deposition. An appropriate pressure was applied to ensure intimate contact between the SWCNTs and the NiO film by using a clamp (Figure S2a, Supporting Information). Finally, the stacked substrates were heated at 350 °C under an ambient atmosphere in a tubular furnace. Because of the different reactivities of m- and s-SWCNTs, m-SWCNTs intend to react with NiO preferentially and be etched during the process. We tried different reaction temperatures and times (Figure S3, Supporting Information) and found that there was no obvious change of the as-grown SWCNTs at a lower reaction temperature of 300 °C; no obvious change to the original SWCNTs occurred as confirmed by SEM observation and laser Raman measurement. While under 400 °C and prolonged reaction time, most of the SWCNTs were destroyed. Thus, the optimum reaction condition was set to be 350 °C and 30 min.

The as-grown SWCNTs and the SWCNTs that remained after the carbothermic reaction were compared using laser Raman spectroscopy with the excitation laser wavelengths of 532 and 633 nm. Figure 2 panels a and c show the laser Raman spectra of the as-grown SWCNTs, in which the radial breathing mode (RBM) peaks originating from s- and m-SWCNTs are highlighted with blue and pink colors, respectively, according to the Kataura plot.[25] It can be seen that both m-SWCNTs and s-SWCNTs coexist in the as-grown SWCNT samples. Figure 2 panels b and d show the results for the SWCNTs obtained after the carbothermic reaction. We can see that most of the RBM peaks assigned to m-SWCNTs disappear, while the peaks originating from s-SWCNTs are mostly retained. The samples were further examined by using an excitation laser wavelength of 785 nm and similar results were obtained (Figure S4, Supporting Information). These results indicate that most of the m-SWCNTs were

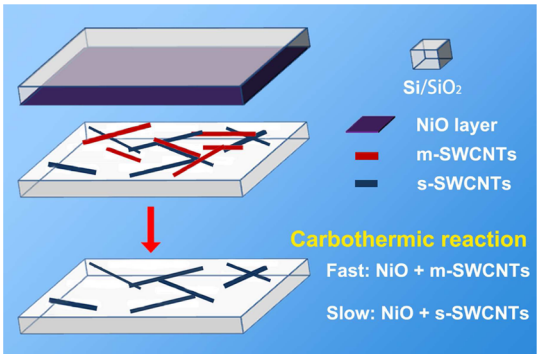

Figure 1. Schematic showing the selective removal of m-SWCNTs by the carbothermic reaction with a NiO thin film.

removed by the carbothermic reaction with NiO and the remaining material is dominated by s-SWCNTs. It should be pointed out that there are still very weak signals originating from m-SWCNTs in Figure 2 panels b and d. It is possible that a limited number of m-SWCNTs survive the carbothermic reaction due to their larger diameter or bundled-structure, which gives them a high oxidation resistance. In order to obtain a higher percentage of s-SWCNTs, it is important to realize precise control over the diameter of SWCNTs. And also, our results showed that the SWCNTs with lower area density usually have a better selectivity.

To verify that the selective etching is realized by the carbothermic reaction, we performed a comparative study in which the as-grown SWCNTs were heat treated at 350 °C in air for 30 min without using any metal oxides. SEM images and laser Raman spectra of the SWCNTs before and after the thermal oxidation showed no obvious difference (Figure S5, Supporting Information), indicating that the structure of the SWCNTs remained almost unchanged. Therefore, it is reasonable to conclude that the NiO thin film plays a key role in the selective removal of m-SWCNTs at such a low temperature.

All-carbon nanoelectronics have attracted intense research interest due to their attractive potential applications in various flexible, transparent devices.[26−28] After selective removal of m-SWCNTs, we further fabricated all-SWCNT FET devices using the obtained s-SWCNTs as the channel material and the as-grown SWCNTs as source/drain electrodes. Figure 3a schematically shows the fabrication process. The patterned NiO strips, rather than a uniform NiO film, were used to selectively remove m-SWCNTs. A schematic showing the contact between the NiO stripes and SWCNTs before and after the carbothermic reaction is shown in Figure S2b (Supporting Information). As a result, the m-SWCNTs (red lines) contacting the NiO strips were selectively removed by the carbothermic reaction, while in the blank areas (free of NiO), the SWCNTs were not affected. The remaining s-SWCNTs were then directly used as the channel material and the intact SWCNTs as the source/drain electrodes. By using

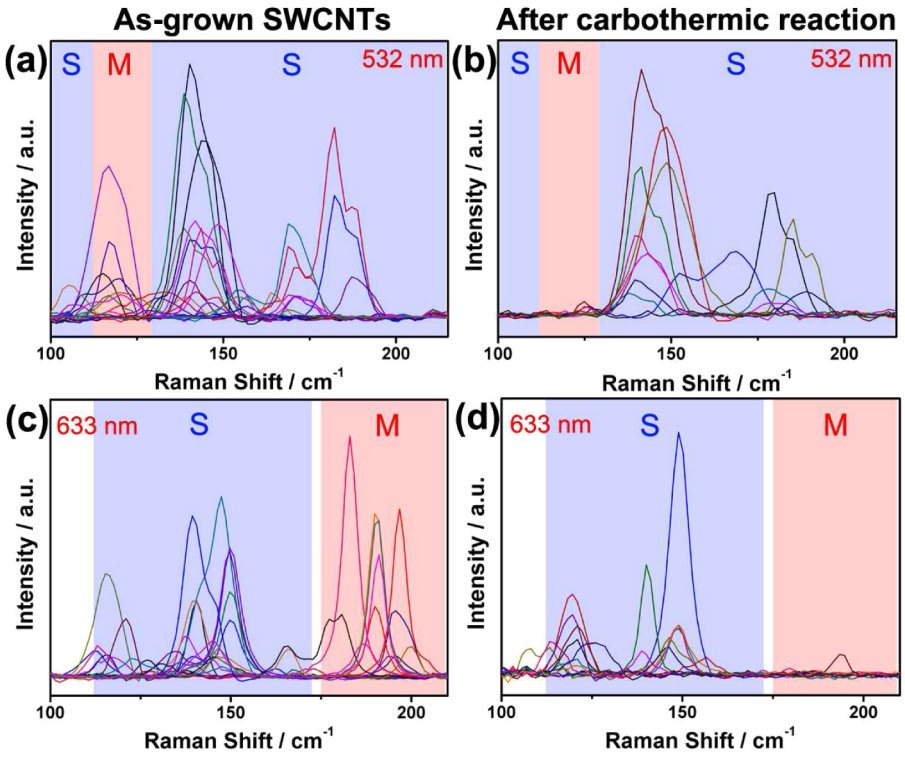

Figure 2. Laser Raman spectra of (a, c) the as-grown SWCNTs and (b, d) the SWCNTs remaining after the carbothermic reaction with NiO with laser excitation wavelengths of (a, b) 532 nm and (c, d) 633 nm. The regions corresponding to semiconducting and metallic transitions are labeled as S (blue) and M (pink), respectively. The baselines of the spectra have been subtracted.

patterned NiO masks, all-SWCNT FETs and even more complicated circuits could be fabricated.

Figure 3b shows a SEM image of the patterned NiO strips with a thickness of ~100 nm, a width of ~10 μm deposited on a Si/SiO_2 substrate by a standard photolithography, metal evaporation, and lift-off process. Figure 3c shows a typical SEM image of the fabricated all-SWCNT FET. It can be seen that the density of SWCNTs in the channel area obviously decreases due to the selective removing of m-SWCNTs and the loss of a part of s-SWCNTs, while the SWCNT serving as source/drain electrodes remains almost unchanged. The residual s-SWCNTs have a shorter average length, but they bridge and connect well with the source/drain SWCNT electrodes. There was no Ni residue detected by either SEM observation or energy dispersive spectrometer analysis.

The electrical measurements of the all-SWCNT FETs were performed using a probe station. The all-SWCNT FETs have typically a channel length of ~10 μm and a channel width of ~500 μm. Two W-tip probes were connected directly with the SWCNT source/drain electrodes. The third probe was connected to the silicon bottom gate electrode. It is worth noting that our device assembly process is quite simple because the conventional deposition process of the metal electrodes is not needed. Moreover, the all-SWCNT configuration avoids possible carbothermic reaction between carbonaceous channel material and the connecting metal electrodes, such as Au, Pt, and Pd, and hence improves the high temperature durability and stability of the FET devices.[24]

Figure 3d compares the transport properties of two typical FET devices. One device was the above-mentioned all-SWCNT FET, and the other was fabricated by transferring an as-grown SWCNT film onto Au/Ti electrodes predeposited on a Si/SiO_2 wafer. The as-grown SWCNT FET showed a low current ON/OFF ratio of ~5, which is consistent with the previous reported results for mixed m- and s-SWCNT devices.[5,9] It can be seen that the source-drain current cannot be turned off by tuning the gate bias, due to the bridging of m-SWCNTs between the electrodes. In contrast, the all-SWCNT FET showed a dramatically improved current ON/OFF ratio of ~10^3, indicating that the channel material is s-SWCNT dominated. Figure 3e shows the statistical results of the I_{on}/I_{off} ratios for the as-grown SWCNT FETs and all-SWCNT FETs. The as-grown SWCNT FETs have small I_{on}/I_{off} ratios ranging from 2 to 8, which can be ascribed to the coexistence of mixed m- and s-SWCNTs. While the all-SWCNT FETs using the s-SWCNTs derived from carbothermic reaction as the channel material show much higher I_{on}/I_{off} ratios; 20% of these FETs have I_{on}/I_{off} ratios larger than 10^3, 34% of the FETs larger than 10^2, and the rest larger than 10. These results further confirm that the carbothermic reaction approach is efficient for selective removal of m-SWCNTs. The mobilities of the as-grown SWCNT FETs were evaluated to be in the range of 10−70 $cm^2/(V\ s)$, and

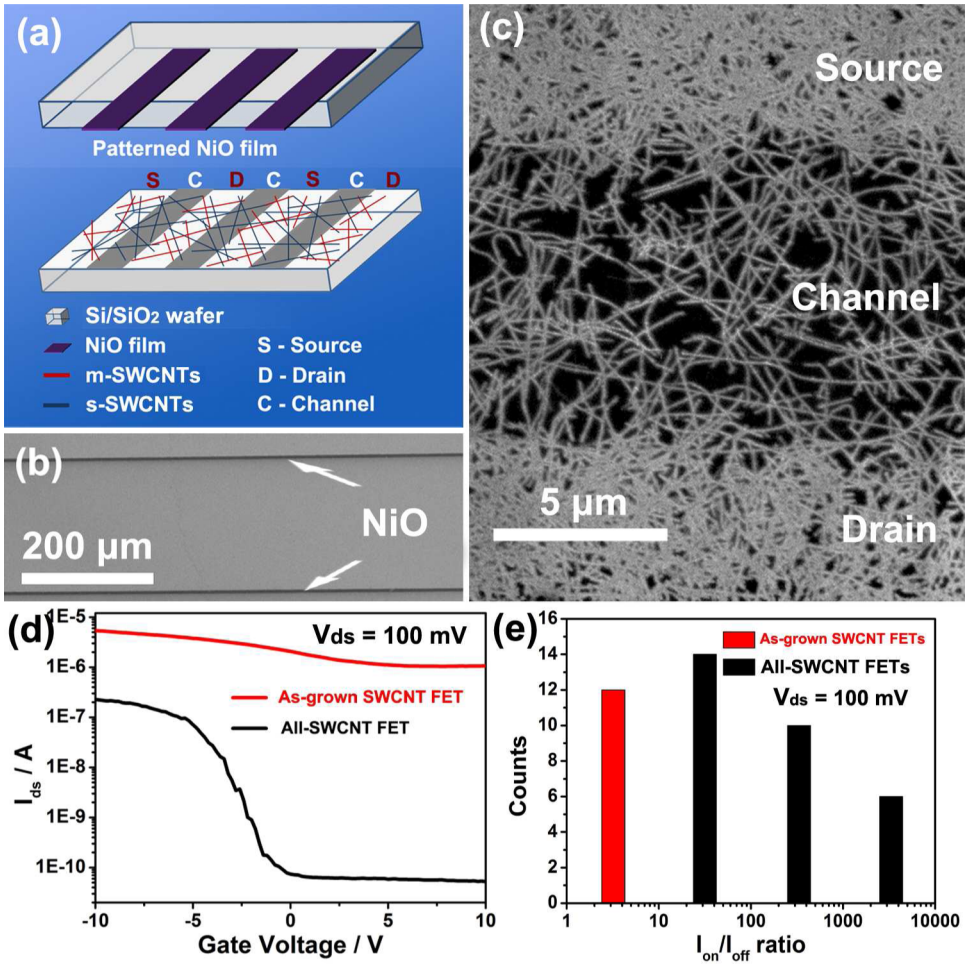

Figure 3. (a) Schematic showing the fabrication process of the all-SWCNT FETs using patterned NiO strips. (b) SEM image of patterned NiO strips with a thickness of ~100 nm and a width of ~10 μm. (c) SEM image showing the source, channel, and drain of an all-SWCNT FET fabricated by the carbothermic reaction with patterned NiO strips. (d) Comparisons of the transport characteristics of the as-grown SWCNT FET and all-SWCNT FET. (e) Histogram showing the statistical I_{on}/I_{off} ratios of the as-grown SWCNT FETs and all-SWCNT FETs.

the all-SWCNT FETs have lower mobilities of 3–20 $cm^2/(V\ s)$ (Figure S6, Supporting Information). This is possibly because of the removal of m-SWCNTs and the decrease of SWCNT length caused by the carbothermic reaction. Using milder carbothermic reaction conditions and appropriate channel width and length may further improve the mobility of the FETs. In this study, we use micrometer-scale NiO strips as an etchant to make FETs. When the dimensions of the NiO pattern are further decreased and its configuration is carefully designed, high density FETs and even complex devices and circuits are expected to be fabricated using this approach.

CONCLUSION

In summary, we have demonstrated for the first time that m-SWCNTs can be selectively removed by a carbothermic reaction at a low temperature with a high efficiency. An all-SWCNT FET was fabricated using intact SWCNTs as source/drain electrodes and the enriched s-SWCNTs as channel material. The all-SWCNT FET showed an improved current ON/OFF ratio of $\sim 10^3$. In combination with their easy fabrication process and good stability, the all-SWCNT FETs may find applications in high-performance, flexible, low-cost electronic devices in future.

METHODS

Carbon Nanotube Synthesis. For SWCNT growth, about 0.1 nm-thick Co film was deposited on a Si/SiO_2 wafer by ion-beam sputtering as a catalyst. The Co film was annealed at 900 °C for 5 min under a mixed Ar (200 sccm) and H_2 (50 sccm) flow. Then, a Ar flow (200 sccm) was introduced to bubble through an ethanol solution (C_2H_5OH/H_2O, 4/1 vol ratio) to start the SWCNT growth. The growth time was 5–10 min.

All-SWCNT FET Fabrication and Testing. A SWCNT film of 500 μm wide and 10 mm long was used as a starting material. After the carbothermic reaction with patterned NiO stripes at 350 °C, FETs with a channel length of 10 μm and channel width of 500 μm were fabricated (Figure S2c, Supporting Information).

The all-SWCNT FETs were tested by using a probe station. A keithley SCS-4200 instrument was used to measure their transport properties by applying a source−drain bias of 0.1 V, with the gate bias scanning from −10 to 10 V with a step of 0.1 V.

Conflict of Interest: The authors declare no competing financial interest.

Acknowledgment. This work was supported by the Ministry of Science and Technology of China (Grant 2011CB932601) and National Natural Science Foundation of China (Grant 50921004). The authors would like to thank Dr. B. L. Liu for helpful discussions.

Supporting Information Available: Illustration showing the fabrication process of the all-SWCNT FETs. SEM image and XPS spectra of the NiO film. SEM images and laser Raman spectra of the SWCNTs under different carbothermic reaction temperatures and time. Laser Raman spectra of the SWCNTs with an excitation wavelength of 785 nm. SEM images and laser Raman spectra of the SWCNTs before and after heat treatment at 350 °C under ambient atmosphere for 30 min. The mobilitites and I_{on}/I_{off} ratio of the as-grown SWCNT FETs and all-SWCNT FETs. This material is available free of charge *via* the Internet at http://pubs.acs.org.

REFERENCES AND NOTES

1. Durkop, T.; Getty, S. A.; Cobas, E.; Fuhrer, M. S. Extraordinary Mobility in Semiconducting Carbon Nanotubes. *Nano Lett* **2004**, *4*, 35–39.
2. Yao, Z.; Kane, C. L.; Dekker, C. High-Field Electrical Transport in Single-Wall Carbon Nanotubes. *Phys. Rev. Lett.* **2000**, *84*, 2941–2944.
3. Liang, W. J.; Bockrath, M.; Bozovic, D.; Hafner, J. H.; Tinkham, M.; Park, H. Fabry−Perot Interference in a Nanotube Electron Waveguide. *Nature* **2001**, *411*, 665–669.
4. Javey, A.; Kim, H.; Brink, M.; Wang, Q.; Ural, A.; Guo, J.; McIntyre, P.; McEuen, P.; Lundstrom, M.; Dai, H. J. High-Kappa Dielectrics for Advanced Carbon-Nanotube Transistors and Logic Gates. *Nat. Mater.* **2002**, *1*, 241–246.
5. Li, Y. M.; Mann, D.; Rolandi, M.; Kim, W.; Ural, A.; Hung, S.; Javey, A.; Cao, J.; Wang, D. W.; Yenilmez, E; *et al.* Preferential Growth of Semiconducting Single-Walled Carbon Nanotubes by a Plasma Enhanced CVD Method. *Nano Lett.* **2004**, *4*, 317–321.
6. Ding, L.; Tselev, A.; Wang, J. Y.; Yuan, D. N.; Chu, H. B.; McNicholas, T. P.; Li, Y.; Liu, J. Selective Growth of Well-Aligned Semiconducting Single-Walled Carbon Nanotubes. *Nano Lett.* **2009**, *9*, 800–805.
7. Hong, G.; Zhang, B.; Peng, B. H.; Zhang, J.; Choi, W. M.; Choi, J. Y.; Kim, J. M.; Liu, Z. F. Direct Growth of Semiconducting Single-Walled Carbon Nanotube Array. *J. Am. Chem. Soc.* **2009**, *131*, 14642–14643.
8. Qu, L. T.; Du, F.; Dai, L. M. Preferential Synthesis of Semiconducting Vertically Aligned Single-Walled Carbon Nanotubes For Direct Use in FETs. *Nano Lett.* **2008**, *8*, 2682–2687.
9. Yu, B.; Liu, C.; Hou, P. X.; Tian, Y.; Li, S. S.; Liu, B. L.; Li, F.; Kauppinen, E. I.; Cheng, H. M. Bulk Synthesis of Large Diameter Semiconducting Single-Walled Carbon Nanotubes by Oxygen-Assisted Floating Catalyst Chemical Vapor Deposition. *J. Am. Chem. Soc.* **2011**, *133*, 5232–5235.
10. Harutyunyan, A. R.; Chen, G. G.; Paronyan, T. M.; Pigos, E. M.; Kuznetsov, O. A.; Hewaparakrama, K.; Kim, S. M.; Zakharov, D.; Stach, E. A.; Sumanasekera, G. U. Preferential Growth of Single-Walled Carbon Nanotubes with Metallic Conductivity. *Science* **2009**, *326*, 116–120.
11. Tanaka, T.; Jin, H.; Miyata, Y.; Fujii, S.; Suga, H.; Naitoh, Y.; Minari, T.; Miyadera, T.; Tsukagoshi, K.; Kataura, H. Simple and Scalable Gel-Based Separation of Metallic and Semiconducting Carbon Nanotubes. *Nano Lett.* **2009**, *9*, 1497–1500.
12. Arnold, M. S.; Green, A. A.; Hulvat, J. F.; Stupp, S. I.; Hersam, M. C. Sorting Carbon Nanotubes by Electronic Structure Using Density Differentiation. *Nat. Nanotechnol.* **2006**, *1*, 60–65.
13. Strano, M. S.; Dyke, C. A.; Usrey, M. L.; Barone, P. W.; Allen, M. J.; Shan, H. W.; Kittrell, C.; Hauge, R. H.; Tour, J. M.; Smalley, R. E. Electronic Structure Control of Single-Walled Carbon Nanotube Functionalization. *Science* **2003**, *301*, 1519–1522.
14. Burghard, M.; Balasubramanian, K.; Sordan, R.; Kern, K. A Selective Electrochemical Approach to Carbon Nanotube Field-Effect Transistors. *Nano Lett.* **2004**, *4*, 827–830.
15. An, L.; Fu, Q. A.; Lu, C. G.; Liu, J. A Simple Chemical Route To Selectively Eliminate Metallic Carbon Nanotubes in Nanotube Network Devices. *J. Am. Chem. Soc.* **2004**, *126*, 10520–10521.
16. Lee, Y. H.; An, K. H.; Park, J. S.; Yang, C. M.; Jeong, S. Y.; Lim, S. C.; Kang, C.; Son, J. H.; Jeong, M. S. A Diameter-Selective Attack of Metallic Carbon Nanotubes by Nitronium Ions. *J. Am. Chem. Soc.* **2005**, *127*, 5196–5203.
17. Collins, P. C.; Arnold, M. S.; Avouris, P. Engineering Carbon Nanotubes and Nanotube Circuits Using Electrical Breakdown. *Science* **2001**, *292*, 706–709.
18. Seidel, R.; Graham, A. P.; Unger, E.; Duesberg, G. S.; Liebau, M.; Steinhoegl, W.; Kreupl, F.; Hoenlein, W. High-Current Nanotube Transistors. *Nano Lett.* **2004**, *4*, 831–834.
19. Vijayaraghavan, A.; Kanzaki, K.; Suzuki, S.; Kobayashi, Y.; Inokawa, H.; Ono, Y.; Kar, S.; Ajayan, P. M. Metal−Semiconductor Transition in Single-Walled Carbon Nanotubes Induced by Low-Energy Electron Irradiation. *Nano Lett.* **2005**, *5*, 1575–1579.
20. Gomez, L. M.; Kumar, A.; Zhang, Y.; Ryu, K.; Badmaev, A.; Zhou, C. W. Scalable Light-Induced Metal to Semiconductor Conversion of Carbon Nanotubes. *Nano Lett.* **2009**, *9*, 3592–3598.
21. Yu, B.; Hou, P. X.; Li, F.; Liu, B. L.; Liu, C.; Cheng, H. M. Selective Removal of Metallic Single-Walled Carbon Nanotubes by Combined *in Situ* and Post-synthesis Oxidation. *Carbon* **2010**, *48*, 2941–2947.
22. Zhang, G. Y.; Qi, P. F.; Wang, X. R.; Lu, Y. R.; Li, X. L.; Tu, R.; Bangsaruntip, S.; Mann, D.; Zhang, L.; Dai, H. J. Selective Etching of Metallic Carbon Nanotubes by Gas-Phase Reaction. *Science* **2006**, *314*, 974–977.
23. Zhang, G. Y.; Qi, P. F.; Wang, X. R.; Lu, Y. R.; Mann, D.; Li, X. L.; Dai, H. J. Hydrogenation and Hydrocarbonation and Etching of Single-Walled Carbon Nanotubes. *J. Am. Chem. Soc.* **2006**, *128*, 6026–6027.
24. Lee, J. H.; Shin, J. H.; Kim, Y. H.; Park, S. M.; Alegaonkar, P. S.; Yoo, J. B. A New Method of Carbon-Nanotube Patterning Using Reduction Potentials. *Adv. Mater.* **2009**, *21*, 1257–1260.
25. Dresselhaus, M. S.; Dresselhaus, G.; Saito, R.; Jorio, A. Raman Spectroscopy of Carbon Nanotubes. *Phys. Rep.* **2005**, *409*, 47–99.
26. Liang, X. L.; Wang, S.; Wei, X. L.; Ding, L.; Zhu, Y. Z.; Zhang, Z. Y.; Chen, Q.; Li, Y.; Zhang, J.; Peng, L. M. Towards Entire-Carbon-Nanotube Circuits: The Fabrication of Single-Walled-Carbon-Nanotube Field-Effect Transistors with Local Multiwalled-Carbon-Nanotube Interconnects. *Adv. Mater.* **2009**, *21*, 1339–1343.
27. Yu, W. J.; Chae, S. H.; Lee, S. Y.; Duong, D. L.; Lee, Y. H. Ultra-Transparent, Flexible Single-Walled Carbon Nanotube Non-volatile Memory Device with an Oxygen-Decorated Graphene Electrode. *Adv. Mater.* **2011**, *23*, 1889–1893.
28. Sangwan, V. K.; Southard, A.; Moore, T. L.; Ballarotto, V. W.; Hines, D. R.; Fuhrer, M. S.; Williams, E. D. Transfer Printing Approach to All-Carbon Nanoelectronics. *Microelectron. Eng.* **2011**, *88*, 3150–3154.